Responses to reviewer #1

Dear Editor and Reviewer #1:

We would like to express our sincere gratitude to the editor and the reviewer for their time and invaluable evaluation on our manuscript, "Optimizing Ammonia Emissions for $PM_{2.5}$ Mitigation: Environmental and Health Co-Benefits in Eastern China" (egusphere-2025-1407). The insightful suggestions have enabled us to significantly improve the quality of our work. We have addressed all comments and have revised the manuscript accordingly. The reviewer comments are presented in blue, our point-by-point responses are in black, and the corresponding revisions in the manuscript are highlighted in red.

Major comments:

1. The authors attribute the ammonia emissions underestimate in the model almost entirely to non-agricultural emissions (Figure 2). However, temporally, the authors put the largest posterior increase in ammonia emissions in spring and summer (Figure 5) when I would expect agricultural emissions to be most important (fertilization time + favorable meteorology). At the same time, your sources are close or overlap in space (Figure 2), especially considering the smoothness of the modeled and observational total column NH_3 (Figure 6). Moreover, because of co-linearity, I am not sure how well the MLR (Eqn 4) can separately fit the alpha and beta parameters and thus separate source sectors. For these reasons, I am skeptical of the source attribution in this study. I am more confident in total ammonia emissions magnitudes.

Response:

We thank the reviewer for this comment. We acknowledge the reviewer's point that the regional changes in agricultural NH_3 emissions between prior and posterior inventories are small. This phenomenon could be explained by the spatial heterogeneity of changes in agricultural emissions. For example, our posterior model results for spring show a decrease in agricultural emissions in Henan, while simultaneously proposing a substantial increase of 242.8 Gg in the Yangtze River Delta region. This regional redistribution could improve the model's ability in better matching with observations.

Therefore, the large rise in total emissions in spring is a combination of these regionally specific agricultural adjustments and a significant, spatially broad increase in the non-agricultural sector. It is also important to note that even with this large non-

AGR correction, agriculture remains the dominant source of emissions in spring in our posterior inventory (accounting for 84.1%), reflecting the overwhelming importance of fertilization activity in this season.

The use of multiple linear regression (MLR) for source apportionment is a well-established approach in atmospheric science (Qi et al., 2024; Shu and Lam, 2011; Trošić Lesar and Filipčić, 2023) and can identify different physical sources. The fundamental principle of using regression for source apportionment is that different sources can be statistically distinguished if they possess unique spatial "fingerprints".

In our study, the high-concentration regions resulting from AGR and non-AGR emissions do not spatially align (Figure R1.1). The overall spatial correlation between the NH_3 columns simulated from these two sources is low (r = 0.35) and is near zero in the high-concentration regions (r = 0.03). This significant dissimilarity provides a robust statistical basis for the MLR model to distinguish their relative contributions.

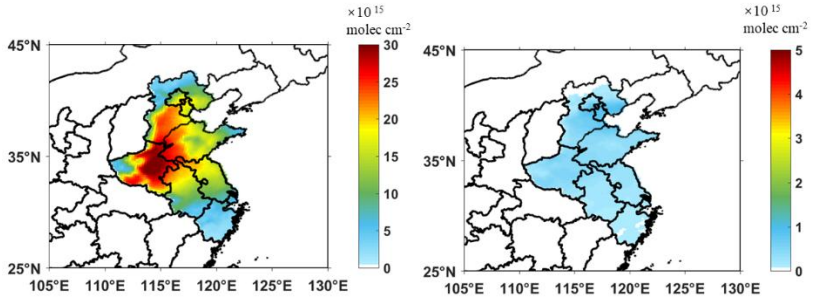

Figure R1.1: Spatial distribution of prior simulated NH_3 column concentrations from agricultural and non-agricultural sources.

Revision in Section 4.1:

In each iterative calculation, the monthly average satellite-derived NH_3 column concentration served as the target, and multiple linear regression (MLR) was applied to calculate the corresponding regression factors for AGR and non-AGR emissions (Figure S3). This separation of sectors by MLR is effective because their respective spatial distributions are distinct and largely uncorrelated (r = 0.35).

Revision in Section 4.2:

In multiple iterations, the framework optimizes the relative mix of the two sources to better match the observed spatial patterns. For instance, the spatial correlation between model and observation in Henan increased from 0.47–0.58 (prior simulations)

to 0.64–0.90 (posterior simulations).

2. The MLR does not account for chemistry occurring between emission and observation. Could you comment on how this affects the results?

Response:

We thank the reviewer for this insightful question, which allows us to clarify the role of atmospheric chemistry within our inversion framework and discuss the associated uncertainties.

First, we emphasize that our methodology inherently accounts for atmospheric chemistry. While the MLR component is a statistical tool, our approach is not a simple regression directly linking emissions to observed columns. Instead, the MLR operates within an iterative framework dynamically coupled with the full WRF-Chem model. Crucially: (1) The inputs to our regression (the SA variables) are the simulated NH_3 column concentrations generated by WRF-Chem. This means that within each iteration, WRF-Chem explicitly simulates all complex, non-linear chemical transformations (including gas-to-particle partitioning and aerosol formation) and transport processes occurring between emission and the resulting atmospheric concentration. (2) The MLR then acts solely as an efficient optimization tool, adjusting the emission inputs based on the outputs of this chemically comprehensive model.

To directly discuss the model's capacity in characterizing concentrations of secondary inorganic aerosols (SIA), we conducted comparisons using in-situ measurements at a representative site in Beijing (39°59′21″N, 116°18′25″E).

The evaluation results are summarized in Table R1. It is revealed that the posterior NH_3 emissions increase NH_4^+ concentration from 4.71 μg m^{-3} to 4.95 μg m^{-3}, which is closer to the observed average (5.69 μg m^{-3}). The simulated mean NO_3^- concentration with 9.59 μg/m^3 also better matches the observed level (9.44 μg m^{-3}).

The WRF-Chem model performs moderately well in capturing the observed SO_4^{2-} concentration (7.74 μg m^{-3}) in both simulations (5.81-5.84 μg m^{-3}). The model underestimation could be attributed to the missing formation mechanism of sulfate such as transition metal ions (TMI)-catalyzed and photosensitized oxidation of SO_2 on aerosol surfaces (Cai et al., 2024; Wang et al., 2021, 2020). Although this underestimation of sulfate might lead to our posterior NH_3 emission estimates being

conservatively low, we find that the model still reproduces the total secondary inorganic aerosol (SIA) concentrations well, with an overall bias of only -11.0%. This good performance in simulating the total aerosol sink for ammonia suggests that the uncertainty propagated to the final emission estimates from these chemical pathways is limited.

In summary, our framework inherently accounts for chemistry through its tight coupling with WRF-Chem. The evaluation against SIA observations confirms the chemical plausibility of our results for nitrate and ammonium, while highlighting specific uncertainties in sulfate chemistry. These uncertainties suggest our posterior NH_3 emissions may represent a conservative estimate. We have incorporated this discussion into the revised manuscript.

Table R1: Comparison of prior and posterior simulated surface concentrations with in-situ observations for major secondary inorganic aerosol components (sulfate, nitrate, and ammonium) in Beijing. All values are in μg m^{-3}.

	Prior simulation	Posterior simulation	observation
nitrate	8.82	9.59	9.44
ammonium	4.71	4.95	5.69
sulfate	5.81	5.84	7.74

Revision in Section 2.2:

Furthermore, speciated inorganic aerosol data from a representative site in Beijing were collected to evaluate the model's capacity in characterizing the formation of secondary inorganic aerosols (Tan et al., 2018).

Revision in Section 4.1:

Finally, the entire process is iteratively repeated, a framework that captures the overall non-linear atmospheric response by combining the dynamic simulation of non-linear chemistry within each WRF-Chem step with the collective behavior of multiple iterations.

Revision in Section 4.2:

Additionally, uncertainties from the model's chemical mechanisms and the

influence of nearby grid transport also contribute to this gap, but the overall impact on the final estimate is limited.

Revision in Section 4.3:

To further characterize the model's chemical performance beyond total $PM_{2.5}$, we also evaluated the simulation of secondary inorganic aerosol (SIA) components against in-situ measurements from a representative site in Beijing (Table S7). The evaluation shows that the posterior NH_3 emissions improved the simulation of ammonium and nitrate, reducing the bias between simulated and observed concentrations. Although the model underestimates sulfate, likely due to missing formation mechanisms (Cai et al., 2024; Wang et al., 2021, 2020), the total SIA concentration is well reproduced with an overall bias of only -11.0%.

Revision in Supplementary:

Table S7. *Comparison between the prior and posterior simulated inorganic aerosol concentrations with in-situ measurements in Beijing. All value units are μg m^{-3}.*

	Prior simulation	*Posterior simulation*	*observation*
nitrate	*8.82*	*9.59*	*9.44*
ammonium	*4.71*	*4.95*	*5.69*
sulfate	*5.81*	*5.84*	*7.74*

Minor comments:

1. Line 75: It is not clear to me what the 1%–50% figure represents here. Is this reduction in $PM_{2.5}$ per unit NH_3 emissions reduced?

Response:

We thank the reviewer for this question. The 1%–50% range in our text is intended to summarize the breadth of these varying findings reported in the studies we referenced. It represents the range of discrepancies or varying outcomes found across the cited literature when assessing the impact of NH_3 emission reductions on $PM_{2.5}$ levels. This variability arises from differences in study methodologies, including models, underlying emission inventories, regions, and seasons analyzed. To enhance clarity, we have revised the relevant sentence in the manuscript to explicitly state that this range reflects the spectrum of outcomes reported in the referenced studies.

Revision in Section 1:

The uncertainty in the emission estimation further contributes to significant discrepancies, reflecting the range of results (1%–50%) reported in the literature, in assessing the impacts of NH_3 reduction on $PM_{2.5}$ level (Guo et al., 2018, 2024; Li et al., 2024; Liu et al., 2019, 2021, 2023; Pan et al., 2024; Zhang et al., 2022).

2. Which version of the IASI NH_3 data do you use?

Response:

We appreciate the reviewer's attention to this detail. We have clarified in the revised text that the IASI NH_3 data used in this study is version 3.0.

Revision in Section 2.2:

We obtained the total column density of NH_3 from the passive satellite remote-sensing product of the Infrared Atmospheric Sounding Interferometer (IASI) (version 3.0, https://iasi.aeris-data.fr/nh3/, last accessed on December 2020) as the observational constraint.

3. Lines 165–166: What do the index of agreement and mean fractional bias mean, intuitively?

Response:

We appreciate the reviewer's suggestion to clarify these metrics. The manuscript now includes expanded intuitive explanations:

(1) Index of Agreement (IOA)

The IOA quantifies the overall simulation skill with values ranging from 0 to 1, where 1 indicates perfect match between simulated and observed data while 0 denotes complete disagreement. This metric evaluates both magnitude accuracy and spatial pattern consistency, making a higher IOA value indicative of better model performance. In our context, an increased IOA in posterior simulations versus prior runs confirms improved representation of NH_3 columns.

(2) Mean Fractional Bias (MFB)

The MFB diagnoses systematic model bias with values centered at 0. A value of 0 signifies no average bias, positive values indicate model overestimation, and negative values reflect underestimation. The absolute magnitude measures bias severity, where smaller absolute values correspond to reduced systematic error.

In this study, we use IOA to evaluate global consistency between simulated and satellite-observed NH_3 columns, while MFB specifically quantifies directional bias tendencies. These clarifications have been incorporated into the revised manuscript.

Revision in Section 3:

The IOA quantifies the overall model skill, where a value of 1 indicates a perfect match and 0 denotes complete disagreement. The MFB diagnoses systematic model bias, where positive values indicate overestimation, negative values indicate underestimation, and 0 signifies no average bias.

4. Line 167: What does the C mean in these equations? I presume ammonia column concentrations?

Response:

We thank the reviewer for highlighting this ambiguity. In the equations, C is defined as the **C**oncentration of the target pollutant, with its specific meaning determined by the evaluation context: (1) NH_3 total column concentrations (satellite comparison); (2) Surface NH_3 concentrations; (3) Other pollutants (e.g., surface $PM_{2.5}$ SO_2, NO_2)

We have revised the manuscript to explicitly clarify this generalized notation and its context-dependent applications.

Revision in Section 3:

They were calculated following Eq. 1~3, where C represents the concentration of the target pollutant (e.g., NH_3 total column or surface concentrations), and subscripts s, o and N represent simulations, observations, and the number of samples, respectively.

5. How do you convert simulated NH_3 to total column densities comparable to IASI (e.g. the SA in line 205)?

Response:

We thank the reviewer for requesting methodological clarification. The conversion of simulated NH_3 to total column densities (SA variables) is now detailed in the Supporting Information.

The WRF-Chem model outputs NH_3 concentrations as a volume mixing ratio (in ppmv) for each model layer. To convert these layer-specific concentrations into a total vertical column density (VCD) comparable to IASI satellite retrievals, the subsequent process was followed.

First, the thickness of each model layer (ΔZ) must be determined. As our WRF-Chem setup uses a terrain-following hybrid sigma-pressure coordinate system, the geopotential height (Z) of each model level is calculated from the model's perturbation geopotential (PH) and base-state geopotential (PHB), divided by the acceleration due to gravity ($g \approx 9.8$ m s^{-2}):

$$Z = \frac{PH + PHB}{g}$$

The thickness of an individual model layer, k, is then the difference in geopotential height between its upper and lower boundaries: $\Delta Z_k = Z_{k+1} - Z_k$

Moreover, the NH_3 volume mixing ratio in each layer is converted to a number density (N_{NH3}, in molecules cm^{-3}), using the pressure and temperature of that specific model layer. Finally, the total NH_3 vertical column density (VCD, in molecules cm^{-2}) is calculated by integrating the vertical column density in each layer of the model. In our discrete model layers, this is achieved by summing the partial column of each layer, which is the product of the number density ($N_{NH3,k}$) and the layer thickness (ΔZ_k).

Revision in Section 3:

The detailed method for calculating NH_3 total column concentrations and surface volume concentrations from WRF-Chem is provided in Text S1.

Revision in Supplementary:

TEXT S1

For comparison with IASI satellite retrievals, the total vertical column density (VCD) was calculated from the model's layer-specific output. The WRF-Chem model outputs NH_3 concentrations as a volume mixing ratio (in ppmv) for each model layer. To convert these layer-specific concentrations into a VCD, the subsequent process was followed.

First, the thickness of each model layer (ΔZ) must be determined. As our WRF-Chem setup uses a terrain-following hybrid sigma-pressure coordinate system, the geopotential height (Z) of each model level is calculated from the model's perturbation geopotential (PH) and base-state geopotential (PHB), divided by the acceleration due to gravity ($g \approx 9.8\ m\ s^{-2}$):

$$Z = \frac{PH + PHB}{g}$$

The thickness of an individual model layer, k, is then the difference in geopotential height between its upper and lower boundaries: $\Delta Z_k = Z_{k+1} - Z_k$

Moreover, the NH_3 volume mixing ratio in each layer is converted to a number density (N_{NH3}, in molecules cm^{-3}), using the pressure and temperature of that specific model layer. Finally, the total NH_3 vertical column density (VCD, in molecules cm^{-2}) is calculated by integrating the vertical column density in each layer of the model. In our discrete model layers, this is achieved by summing the partial column of each layer, which is the product of the number density ($N_{NH3,k}$) and the layer thickness (ΔZ_k).

6. Figure 3: What does the red box represent?

Response:

We appreciate this suggestion to enhance figure clarity. The red box highlights the range we consider to represent good model performance. Specifically, it delineates the area where the Root Mean Square Error (RMSE) is less than 10, and the ratio of simulated-to-observed NH_3 column concentration is between 0.7 and 1.3 (±30% error margin). We have added this clarification to the figure caption in the revised manuscript.

Revision in Section Figure 3:

Figure 3. *Scatter plots of the prior and posterior NH_3 total column data versus*

IASI retrievals. Each point represents prior (or posterior) data for a specific season and a specific region. Circles, triangles, rhombuses, and rectangles correspond to the BTH, Henan, Shandong, and YRD regions, respectively. Orange and blue markers represent a prior and a posterior data, respectively. The red box indicates the performance area, with a model error within ±30% and an RMSE below 10($\times 10^{15}$ molec cm^{-2}).

7. Line 214: What is A_blank? Also, what are these A variables more generally? They are not defined.

Response:

Thank you for this question, which allows us to clarify these important methodological details. To clarify, the A variables (e.g., A_{agr}, $A_{non\text{-}agr}$) represent the total simulated NH_3 column concentrations that result from each of the sensitivity simulations listed in Table 2.

Specifically, The A_{blank} case refers to a simulated NH_3 total column in which all anthropogenic emissions within the study domain were turned off. The purpose of this simulation was to establish a blank line concentration field, which represents the influence of the chemical boundary conditions provided to our model domain.

We have revised the manuscript to provide explicit definitions.

Revision in Section 4.1:

The $SA_{agriculture}{}_{i-1}^{j,k}$, $SA_{non-agriculture}{}_{i-1}^{j,k}$, and $SA_{transport}{}^{j,k}$ are calculated by subtracting A_{blank} from A_{agr}, $A_{non\text{-}agr}$, and $A_{transport}$, respectively. Here, symbols A represent the total simulated NH_3 column concentrations that result from each of the sensitivity simulations listed in Table 1. Specifically, the modeling case A_{blank} refers to a simulated NH_3 total column in which all anthropogenic emissions within the study domain were zeroed out. The purpose of this simulation was to establish background concentrations, which represents the influence of the chemical boundary conditions provided to our model domain.

8. Equation 4: The SA variables are referring to simulated values, right? This is not clear.

Response:

We confirm that the SA variables in Equation 4 represent simulated NH_3 column

concentrations from specific source categories. We have revised the manuscript to explicitly state this definition and eliminate ambiguity.

Revision in Section 4.1:

where, $TA_{satellite}{}^{j,k}$ denotes the monthly average of total NH_3 column density retrieved from the IASI satellite data, and $SA_{transport}{}^{j,k}$, $SA_{agriculture}{}_{i-1}^{j,k}$ and $SA_{non-agriculture}{}_{i-1}^{j,k}$ stand for the simulated total column concentration of NH_3 contributed by AGR emissions, non-AGR emissions, and outside transportation, respectively.

9. Line 219: How is D_i^j,k calculated, in terms of the variables already given?

Response:

Thank you for this question regarding the specific details of our methodology. The variable $D_i^{j,k}$ represents the relative bias between the total simulated NH_3 column concentration and the satellite-retrieved observation for a given iteration, month, and region. It is calculated as the difference between the mean simulated column and the mean satellite retrieval column, normalized by the mean satellite retrieval column.

Revision in Section 4.1:

we need to correct for this regression coefficient. The biases between the model simulation and the satellite retrievals were calculated as $D_i{}^{j,k}$. Specifically, it is the difference between the mean simulated column and the mean satellite retrieval, divided by the mean satellite retrieval.

10. Line 221: What do you mean by “excessive residuals”? What is the judgement coefficient and how is it calculated?

Response:

We thank the reviewer for highlighting this key quality control aspect. We have revised the manuscript to provide these specific details.

In our regression analysis, a residual is defined as the difference between the observed value (i.e., the satellite-derived NH_3 column) and the value predicted by the MLR model. To objectively identify what we termed "excessive residuals," we utilize the 95% confidence interval of the residual for each individual fit.

Our criterion is as follows: if the 95% confidence interval of a residual does not

contain zero, such a case is flagged as having an "excessive residual." This means the linear model provides a poor fit for that specific data point, and the resulting regression coefficients are deemed unreliable. Consequently, these coefficients are rejected and not used for the emission update in that iteration. In the following Figure R1.2, we can see that red represents outliers and needs to be discarded.

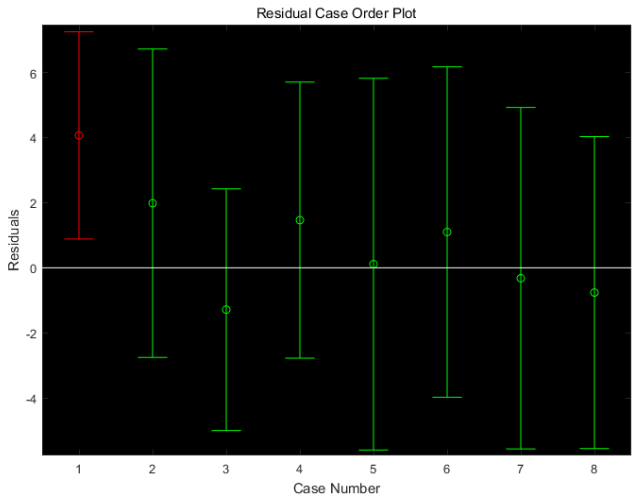

Figure R1.2: Distribution of residuals and their 95% confidence intervals. Each point represents the residual value for a given sample, and the error bars represent the 95% confidence interval of the residual. Green points represent valid fits, while red points are outliers rejected based on the criterion that their confidence interval does not contain zero.

Revision in Section 4.1:

The regression coefficients with excessive residuals, defined as cases where the 95% confidence interval of the residual does not contain zero, are removed to increase credibility.

11. Line 222: What goodness of fit test/metric do you use? How did you pick this 0.3–1 acceptability range?

Response:

We thank the reviewer for requesting methodological clarification. The "goodness of fit" metric we used is the coefficient of determination, commonly known as R-squared (R^2). The R^2 value quantifies the proportion of the variance in the dependent variable that is predictable from the independent variables (the simulated NH_3 columns from AGR and non-AGR sources). This metric ranges from 0 to 1, with higher values

indicating superior model performance.

The acceptability range of 0.3–1 was chosen as a practical criterion within our iterative framework. We established this criterion because regressions with $R^2 < 0.3$ exhibit insufficient explanatory power (indicating >70% unexplained variance), which introduces destabilizing noise into emission adjustments. By excluding such statistically unreliable results from our inventory updates, we maintain algorithm stability while reducing required iteration cycles.

We have now explicitly stated in the manuscript that the metric used is R-squared and have clarified the purpose of this threshold.

Revision in Section 4.1:

Concurrently, the goodness of fit of the regression is calculated as the coefficient of determination (R-square, R^2). To maintain algorithm stability, regressions with an R^2 less than 0.3 are deemed invalid and excluded from the emission update, as they exhibit insufficient explanatory power (indicating >70% unexplained variance) and introduce destabilizing noise into the adjustments.

12. How do you perform the iterations (lines 226-229)? I presume you increment agricultural and non-agricultural emissions for each grid cell by following the fitted alpha and beta parameters, but how exactly and by what magnitude? What do you do for the next increment in the case where you reject the MLR results?

Response:

We appreciate the opportunity to clarify our iterative optimization procedure. The revised manuscript now details this process in Section 4.1.

The iteration is performed by sequentially updating the emission inventory and re-running the WRF-Chem simulation to produce a new concentration field. The magnitude of the emission update in each step is determined by the final adjustment factors (a and b) derived from our corrected MLR analysis. These factors are used as direct scaling multipliers for the emissions. For instance, in the event of the analysis determining a final adjustment factor of 1.3 for the agricultural sector, the new agricultural emission will be set to 1.3 times the value of the previous iteration.

Regarding the case where the MLR results for an iteration are rejected, the process is designed to be conservative. In such instances, the adjustment factors for that specific

grid cell are considered invalid, and the emissions are kept unchanged from the previous iteration. The algorithm then proceeds using this unadjusted emission value as the input for the next step. We have added these specific details about the emission update procedure to the methodology section of our manuscript to improve its clarity.

Revision in Section 4.1:

If a regression is valid, the adjustment factors a and b are set to the new regression coefficients; if invalid, the factors are kept unchanged from the previous iteration. The updated emissions for the next iteration are then calculated by multiplying the emissions from the previous step by these adjustment factors.

13. What does Figure 5 look like if you split the prior and posterior bar plots up into AGR and nonAGR emissions? I am curious about how the source attribution varies with season.

Response:

We thank the reviewer for this valuable suggestion to enhance seasonal attribution analysis. As suggested, we have generated a supplementary figure (Figure S6) decomposing prior and posterior emissions into agricultural (AGR) and non-agricultural (non-AGR) sources by season.

As the new figure illustrates, the source attribution varies significantly by season. Agricultural emissions are the dominant contributor during the spring and summer months, which is consistent with the timing of fertilizer application and higher temperatures that promote volatilization. In contrast, the relative contribution from non-agricultural sources increases substantially in the winter. This winter increase is largely attributed to higher emissions from fossil fuel combustion and other industrial activities that are more pronounced during the cold season.

Revision in Section 4.2:

At the specific-source scale (Figure S6), AGR NH_3 emissions show similar seasonal patterns with the total NH_3 emissions, higher in summer and spring. In contrast, non-AGR NH_3 are highest in winter and fall because fossil fuel combustion-related emissions are higher in cold season, while the lowest emissions occur in summer.

Revision in Supplementary:

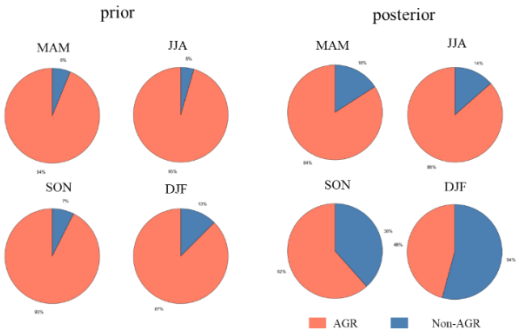

Figure S5: Seasonal comparison of prior and posterior NH_3 emissions from AGR and non-AGR sources.

14. Line 291: What are the units of the RMSE? Is this referring to surface observations or satellite columns?

Response:

Thank you for your detailed review. The units for the RMSE are consistent with the units of the quantities being compared. Therefore, the RMSE has units of molecules cm^{-2} when evaluating against satellite total columns, and units of $\mu g\ m^{-3}$ when evaluating against surface concentration measurements. We have revised the manuscript to explicitly state the appropriate units in each instance to avoid ambiguity.

Revision in Section 4.3:

More than 80% of the points fall in the range where the simulation-to-observation ratio is between 0.7 and 1.3 and the RMSE is less than 10×10^{15} molec cm^{-2}.

Typographical comments:

1. Line 52: Figure should read "55.0%"

Response: Thank you. The text has been corrected as suggested.

Revision in Section 1:

Ammonia (NH_3), a key precursor of $PM_{2.5}$, neutralizes sulfuric acid (H_2SO_4) and nitric acid (HNO_3), leading to the formation of secondary inorganic aerosols (SIA), which contributes 19.4%–55.0% of the total $PM_{2.5}$ (Huang et al., 2014; Liu et al., 2022b; Wang et al., 2016; Wei et al., 2023; Zheng et al., 2015; Zhou et al., 2022).

2. Throughout: the en dash (–) should be used for numerical ranges instead of the tilde (~).

Response: We thank the reviewer for this helpful comment, and the manuscript has been revised accordingly.

3. Lines 179–180: this sentence ends abruptly (what is the RMSE of 10 referring to; what are its units).

Response: Thank you for the comment. The units for the Root Mean Square Error (RMSE) are the same as those for the NH_3 column concentration ($\times 10^{15}$ molec cm^{-2}). We have revised the sentence in the manuscript to include the appropriate units.

Revision in Section 3:

Most simulated NH_3 total column concentrations are underestimated by more than 30% compared with the observed values by satellite with the associated RMSE exceeding 10×10^{15} molec cm^{-2}.

4. Line 226: I presume you mean alpha and beta as in Equation 4, not a and b here?

Response:

Thank you for this comment. In our methodology, α and β are the initial regression coefficients derived directly from the Multiple Linear Regression (MLR) in each iterative step. In contrast, 'a' and 'b' represent the final, corrected adjustment factors that are used to update the emission inventory.

These final factors (a, b) are derived from the initial coefficients (α, β) after a correction process that accounts for the goodness of fit and regression residuals. We have updated the methodology section to explicitly define 'a' and 'b' and to better describe how these adjustment factors are obtained. This clarification should improve

the reader's understanding of our method.

Revision in Section 4.1:

If a regression is valid, the adjustment factors a and b are set to the new regression coefficients; if invalid, the factors are kept unchanged from the previous iteration.

References

Cai, S., Liu, T., Huang, X., Song, Y., Wang, T., Sun, Z., Gao, J., and Ding, A.: Important Role of Low Cloud and Fog in Sulfate Aerosol Formation During Winter Haze Over the North China Plain, Geophysical Research Letters, 51, e2023GL106597, https://doi.org/10.1029/2023GL106597, 2024.

Guo, H., Otjes, R., Schlag, P., Kiendler-Scharr, A., Nenes, A., and Weber, R. J.: Effectiveness of ammonia reduction on control of fine particle nitrate, Atmospheric Chemistry and Physics, 18, 12241–12256, https://doi.org/10.5194/acp-18-12241-2018, 2018.

Guo, Y., Zhang, L., Winiwarter, W., Van Grinsven, H. J. M., Wang, X., Li, K., Pan, D., Liu, Z., and Gu, B.: Ambitious nitrogen abatement is required to mitigate future global PM2.5 air pollution toward the World Health Organization targets, One Earth, 7, 1600–1613, https://doi.org/10.1016/j.oneear.2024.08.007, 2024.

Li, B., Liao, H., Li, K., Wang, Y., Zhang, L., Guo, Y., Liu, L., Li, J., Jin, J., Yang, Y., Gong, C., Wang, T., Shen, W., Wang, P., Dang, R., Liao, K., Zhu, Q., and Jacob, D. J.: Unlocking nitrogen management potential via large-scale farming for air quality and substantial co-benefits, National Science Review, 11, nwae324, https://doi.org/10.1093/nsr/nwae324, 2024.

Liu, M., Huang, X., Song, Y., Tang, J., Cao, J., Zhang, X., Zhang, Q., Wang, S., Xu, T., Kang, L., Cai, X., Zhang, H., Yang, F., Wang, H., Yu, J. Z., Lau, A. K. H., He, L., Huang, X., Duan, L., Ding, A., Xue, L., Gao, J., Liu, B., and Zhu, T.: Ammonia emission control in China would mitigate haze pollution and nitrogen deposition, but worsen acid rain, Proc Natl Acad Sci U S A, 116, 7760–7765, https://doi.org/10.1073/pnas.1814880116, 2019.

Liu, Z., Zhou, M., Chen, Y., Chen, D., Pan, Y., Song, T., Ji, D., Chen, Q., and Zhang, L.: The nonlinear response of fine particulate matter pollution to ammonia emission reductions in North China, Environmental Research Letters, https://doi.org/10.1088/1748-9326/abdf86, 2021.

Liu, Z., Rieder, H. E., Schmidt, C., Mayer, M., Guo, Y., Winiwarter, W., and Zhang, L.: Optimal reactive nitrogen control pathways identified for cost-effective PM2.5 mitigation in Europe, Nat Commun, 14, 4246, https://doi.org/10.1038/s41467-023-39900-9, 2023.

Pan, D., Mauzerall, D. L., Wang, R., Guo, X., Puchalski, M., Guo, Y., Song, S., Tong, D., Sullivan, A. P., Schichtel, B. A., Collett, J. L., and Zondlo, M. A.: Regime shift in secondary inorganic aerosol formation and nitrogen deposition in the rural United States, Nat. Geosci., 17, 617–623, https://doi.org/10.1038/s41561-024-01455-9, 2024.

Qi, L., Zheng, H., Ding, D., and Wang, S.: A comparison of meteorological

normalization of PM2.5 by multiple linear regression, general additive model, and random forest methods, Atmospheric Environment, 338, 120854, https://doi.org/10.1016/j.atmosenv.2024.120854, 2024.

Shu, Y. and Lam, N. S. N.: Spatial disaggregation of carbon dioxide emissions from road traffic based on multiple linear regression model, Atmospheric Environment, 45, 634–640, https://doi.org/10.1016/j.atmosenv.2010.10.037, 2011.

Tan, T., Hu, M., Li, M., Guo, Q., Wu, Y., Fang, X., Gu, F., Wang, Y., and Wu, Z.: New insight into PM2.5 pollution patterns in Beijing based on one-year measurement of chemical compositions, Science of The Total Environment, 621, 734–743, https://doi.org/10.1016/j.scitotenv.2017.11.208, 2018.

Trošić Lesar, T. and Filipčić, A.: Prediction of the SO2 Hourly Concentration for Sea Breeze and Land Breeze in an Urban Area of Split Using Multiple Linear Regression, Atmosphere, 14, 420, https://doi.org/10.3390/atmos14030420, 2023.

Wang, W., Liu, M., Wang, T., Song, Y., Zhou, L., Cao, J., Hu, J., Tang, G., Chen, Z., Li, Z., Xu, Z., Peng, C., Lian, C., Chen, Y., Pan, Y., Zhang, Y., Sun, Y., Li, W., Zhu, T., Tian, H., and Ge, M.: Sulfate formation is dominated by manganese-catalyzed oxidation of SO2 on aerosol surfaces during haze events, Nat Commun, 12, https://doi.org/10.1038/s41467-021-22091-6, 2021.

Wang, X., Gemayel, R., Hayeck, N., Perrier, S., Charbonnel, N., Xu, C., Chen, H., Zhu, C., Zhang, L., Wang, L., Nizkorodov, S. A., Wang, X., Wang, Z., Wang, T., Mellouki, A., Riva, M., Chen, J., and George, C.: Atmospheric Photosensitization: A New Pathway for Sulfate Formation, Environ. Sci. Technol., 54, 3114–3120, https://doi.org/10.1021/acs.est.9b06347, 2020.

Zhang, Z., Yan, Y., Kong, S., Deng, Q., Qin, S., Yao, L., Zhao, T., and Qi, S.: Benefits of refined NH3 emission controls on PM2.5 mitigation in Central China, Sci Total Environ, 814, 151957, https://doi.org/10.1016/j.scitotenv.2021.151957, 2022.